JOURNAL OF COMPUTATIONAL PHYSICS 68, 378–392 (1987)

Supersonic Inviscid Flow— A Three-Dimensional Characteristics Approach

JEFFERSON FONG*

Supercomputer Computations Research Institute, Florida State University, Tallahassee, Florida 32304–4052

AND

LAWRENCE SIROVICH†

Division of Applied Mathematics, Brown University, Providence, Rhode Island

Received September 18, 1985; revised April 25, 1986

Supersonic inviscid flow over nonaxisymmetric bodies is considered. A new version of the method of reference planes is used. In this version, a near characteristics–streamlines coordinate system and a highly efficient numerical integration scheme is developed. The CFL condition is rigorously satisfied on the flow. Several sample calculations are presented.

1. INTRODUCTION

The method of characteristics for three-dimensional flows has been developed in a number of ways. Surveys of this method have been given [1, 2, 3], and the leading approaches have been compared [4]. The main advantages of such methods lie in their intrinsic use of characteristics as well as their accurate calculation of shockwaves. Generally these methods, which require consideration of characteristic conoids and bicharacteristics, are regarded as complex and computationally inefficient compared to the more popular finite difference shock capturing and shock fitting methods, e.g., [5, 6, 7].

Another class of schemes allied to the characteristics method but much simpler to apply is generically referred to as reference plane methods [8–12, 1]. Another designation is method of near characteristics, a terminology which reflects the idea that characteristics are employed in an approximate fashion. In this paper we apply

* Work supported in part by grants from the National Science Foundation (CHE-83-04021) and the U.S. Department of Energy (DE-FC05-85ER25000).

† Work supported by the Air Force Office of Scientific Research (AFOSR 5-28320).

0021-9991/87 $3.00

a variant of this approach to the problem of flow past nonaxisymmetric bodies. Our approach is most closely related to that of Sauer [9] and Rakich [12].

For the case treated here, flow past a body is divided into a set of azimuthal planes. In each plane a highly successful two-dimensional characteristics method [13, 14] is applied. The "cross-talk" between such planes created by azimuthal derivatives and velocities then serve as forcing terms in the equations. Unlike earlier treatments that we are familiar with we are able to rigorously consider domains of dependence follow the Courant–Friedrichs–Lewy (CFL) condition. The result is a method which is extremely fast without loss of efficiency or accuracy.

2. Formulation

Since the form of the governing equations is not standard, we now outline their development. Flow in cylindrical coordinates (x, r, ϕ) is governed by the following equations:

$$\nabla \cdot (\rho \mathbf{u}) = 0, \tag{1}$$

$$v\frac{\partial u}{\partial r} + u\frac{\partial u}{\partial x} = \frac{-w}{r}\frac{\partial u}{\partial \phi} - \frac{1}{\rho}\frac{\partial p}{\partial x}, \tag{2}$$

$$v\frac{\partial v}{\partial r} + u\frac{\partial v}{\partial x} = \frac{-w}{r}\frac{\partial v}{\partial \phi} + \frac{w^2}{r} - \frac{1}{\rho}\frac{\partial p}{\partial r}, \tag{3}$$

$$v\frac{\partial w}{\partial r} + u\frac{\partial w}{\partial x} = \frac{-w}{r}\frac{\partial w}{\partial \phi} - \frac{vw}{r} - \frac{1}{\rho r}\frac{\partial p}{\partial \phi}. \tag{4}$$

In addition to the continuity (1) and momentum equations (2), (3), (4), we have Bernoulli's relation

$$\frac{u^2 + v^2 + w^2}{2} + \frac{a^2}{\gamma - 1} = \frac{M_0^2}{2} + \frac{1}{\gamma - 1}. \tag{5}$$

The gas is specified by the state equation

$$\frac{p}{\rho^\gamma} e^{-(\gamma - 1)S} = \text{constant}, \tag{6}$$

where the entropy S satisfies

$$\mathbf{u} \cdot \nabla S = 0, \tag{7}$$

between shocks while (5) is also valid across shocks [15]. We normalize u, v, w, and the speed of sound a by the upstream speed of sound a_0; x, r by the body length; ρ by its upstream value ρ_0; p by γp_0; and S is replaced by $(S - S_0)/R$, where R is the universal gas constant.

We introduce

$$\theta(x, r, \phi) = \tan^{-1}\left(\frac{v}{u}\right), \tag{8}$$

the flow deflection angle in the projected plane, $\phi = \text{constant}$. Similarly

$$\mu(x, r, \phi) = \sin^{-1}\left(\frac{1}{M_*}\right) \tag{9}$$

is the projected flow Mach angle, where

$$M_*^2 = \frac{u^2 + v^2}{a^2}. \tag{10}$$

In Appendix A it is shown

$$d_\pm(\theta \pm P(\mu)) = \pm\frac{\sin 2\mu}{2}\left(\frac{d_\pm S}{\gamma} - \frac{d_\pm W}{\gamma - 1}\right) + \frac{G_1 \mp (\tan\theta \tan\mu + G_2)}{\tan\theta \pm \tan\mu}\frac{d_\pm r}{r}, \tag{11}$$

where

$$C^\pm: d_\pm = \frac{\partial}{\partial x} + \tan(\theta \pm \mu)\frac{\partial}{\partial r} \tag{12}$$

denotes differentiation in the $C^\pm$-directions, i.e., in the near characteristic directions. $\theta \pm P(u)$ are the corresponding "Riemann invariants." The various terms appearing in (11) are defined in Appendix A. In what follows we also use

$$\sigma = \ln p = \frac{\gamma}{\gamma - 1}\ln\left(1 + \frac{\gamma - 1}{2}M_0^2\right)\Big/\left(1 + \frac{\gamma - 1}{2}\frac{1 + \omega^2}{\sin^2\mu}\right) - S - \ln\gamma, \tag{13}$$

where $\omega = w/q$. The second form for σ in (13) follows from (5) and (6). It should be noted that for axisymmetric flow, we have $\omega = \theta_\phi = \sigma_\phi = 0$, and (11) reduces to the appropriate axisymmetric equations.

Next we define new coordinates (α, β, ζ) such that

$$r_\alpha = x_\alpha \tan(\theta + \mu), \qquad r_\beta = x_\beta \tan\theta, \zeta = \phi. \tag{14}$$

This mapping is further fixed by the condition at the body

$$x(\alpha = 0, \beta, \zeta) = \beta, \tag{15}$$

and the condition that the shock have unit slope at each constant ζ plane, i.e.,

$$\frac{\partial \alpha}{\partial \beta} = 1 \tag{16}$$

at the shock. Under this transformation the C^+ form of (11) becomes

$$R_\alpha^+ = \frac{\sin 2\mu}{2}\left(\frac{S_\alpha}{\gamma} - \frac{W_\alpha}{\gamma - 1}\right) + \frac{G_1 - (\tan\theta \tan\mu + G_2)\, r_\alpha}{\tan\theta + \tan\mu}\frac{}{r}, \tag{17}$$

while the C^- form

$$DR^- = \frac{-\sin 2\mu}{2}\left(\frac{DS}{\gamma} - \frac{DW}{\gamma - 1}\right) + \frac{G_1 + \tan\theta \tan\mu + G_2}{\tan\theta - \tan\mu}\frac{Dr}{r}, \tag{18}$$

where differentiation in C^- direction is now given by,

$$D = \frac{\partial}{\partial \alpha} - \frac{2\tan\theta}{\tan\theta + \tan\mu}\frac{r_\alpha}{r_\beta}\frac{\partial}{\partial \beta}.$$

As shown in Appendix B the ϕ and ζ derivatives are related by

$$\frac{\partial}{\partial \phi} = \frac{(r_\zeta - \tan\theta\, x_\zeta)\, x_\beta (\partial/\partial\alpha) + (\tan(\theta + \mu)\, x_\zeta - r_\zeta)\, x_\alpha (\partial/\partial\beta)}{(\tan\theta - \tan(\theta + \mu))\, x_\alpha x_\beta} + \frac{\partial}{\partial \zeta}. \tag{19}$$

If we combine (17) and (18), then

$$R_\beta^- = (1 - \tan\theta \tan\mu)\frac{x_\beta}{x_\alpha}\frac{\sin 2\mu}{2}\left[\frac{S_\alpha}{\gamma} - \frac{W_\alpha}{\gamma - 1} + (F(\mu))_\alpha\right] + \frac{x_\beta}{r}G_1 + \frac{\sin 2\mu}{2}\left(\frac{W_\beta}{\gamma - 1} - \frac{S_\beta}{\gamma}\right), \tag{20}$$

where

$$F(\mu) = -2\int^\mu \frac{P'(\mu)}{\sin 2\mu}\, d\mu = \frac{1}{\gamma - 1}\ln\left(1 + \frac{\gamma - 1}{2\sin^2\mu}\right).$$

The entropy equation as shown in Appendix A is now

$$S_\beta = \frac{-\omega}{r\cos\theta} S_\phi x_\beta, \tag{21}$$

while the ϕ component of the momentum equation is

$$\frac{\sin^2\mu}{\gamma r}\sigma_\phi+\frac{\cos\theta}{x_\beta}\omega_\beta+\frac{\omega}{r}\omega_\phi$$
$$=\frac{\omega\sin^2\mu\cos\theta}{\gamma}\frac{}{x_\beta}\sigma_\beta-(1+\omega^2)\frac{\omega}{r}\sin\theta. \tag{22}$$

With the use of (13) σ can be eliminated from (22) to give

$$\omega_\beta=\omega\tan\mu P_\beta-\frac{x_\beta}{r\cos\theta}(\omega\sin\theta+\tan\mu P_\phi)$$
$$+\frac{\tan^2\mu}{1+\tan^2\mu}\left[\frac{x_\beta}{r\cos\theta}\left(\frac{S_\phi}{\gamma}-\frac{W_\phi}{\gamma-1}\right)+\omega\left(\frac{W_\beta}{\gamma-1}-\frac{S_\beta}{\gamma}\right)\right]$$
$$-\frac{x_\beta}{r\cos\theta}\omega(\omega_\phi+\omega^2\sin\theta). \tag{23}$$

The dependent variables x, r, θ, μ, ω, and S are determined by (14), (17), (18) or (20), (21), and (23). On the body x, r, θ are specified by the boundary conditions

$$x(\alpha=0,\beta,\zeta)=\beta, \tag{24}$$
$$r(\alpha=0,\beta,\zeta)=f(\beta,\zeta), \tag{25}$$
$$\theta(\alpha=0,\beta,\zeta)=\tan^{-1}\left(\frac{\partial f}{\partial\beta}(\beta,\zeta)\right). \tag{26}$$

In addition to the shock conditions, we also apply (16) at the shock.

3. Numerical Procedures

The following scheme is an extension of the one used in the axisymmetric case [13]. Each azimuthal section ($\zeta_k=$ constant; $k=1,2,...$) has the (α,β) grid shown in Fig. 1. In the neighborhood of the tip, $0\leqslant\beta\leqslant\beta_1$, the flow is taken as flow past a cone, not necessarily circular. For $\beta>\beta_1$ a marching scheme described next is used.

Regard the flow as determined for all columns up to $\beta=\beta_n$ for all ζ_k sections. We first indicate how the flow is determined at the body of the β_n column, denoted by a_1 in Fig. 1. When integrating in the C^- direction as it explicitly appears in (18), we trace this near characteristic back to the β_{n-1} column, the point b_1 in Fig. 1. Flow variables at b_1 are found by a second order accurate interpolation scheme. ζ derivatives are taken as the averages of the center differences at a_1 and at b_1. All other equations are integrated by appropriate elementary grid points differences since they only involve α and β derivatives. The values of the flow for the entire row ζ_k, $k=1,...,$ of body points are now iterated until a convergence criterion is met.

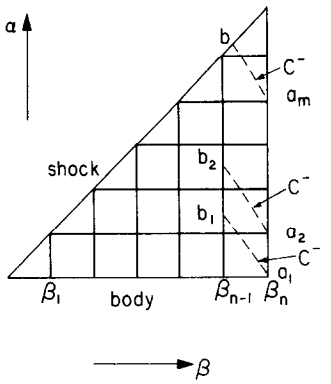

FIG. 1. (α, β) coordinates.

Above the body, instead of the boundary conditions (14)–(26) we have (14), (17). Again values for an entire row are iterated together. We proceed in this manner until the point a_m of Fig. 1 is reached. At this point the C^- near characteristic strikes the shock before hitting the β_{n-1} column. All remaining rows in β_n are now iterated simultaneously.

To consider stability denote the true Mach angle by $\bar{\mu}$. It then follows that

$$\sin^2 \bar{\mu} = \frac{a^2}{q^2 + w^2} = \frac{\sin^2 \mu}{1 + \omega^2},$$

and hence

$$\bar{\mu} \lesssim \mu.$$

At each constant ζ plane, the true domain of dependence for the flow projected onto that plane lies inside the domain of dependence determined by the two near characteristics. As for the ζ derivatives, let b in Fig. 2 be the point to be considered, and let ξ_1 and ξ_2 be the angles (in (x, r, ϕ) space) between $\mathbf{r}_{ab}$ and $\mathbf{r}_{bc}$ and between $\mathbf{r}_{ab}$ and $\mathbf{r}_{bd}$. We want $\xi_1 \geqslant \bar{\mu}$ and $\xi_2 \geqslant \bar{\mu}$. This requirement is easily satisfied unless the aspect ratio (the ratio of the largest to the smallest radius at the cross section) is large, in which case a smaller step size of β is required.

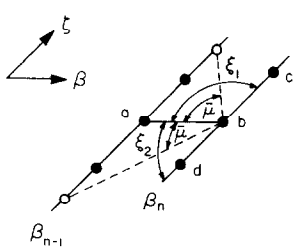

FIG. 2. (β, ζ) coordinates with corresponding angular value in (x, r, ϕ) space.

Some mention of the calculation over a noncircular cone is ordered. Near the tip ($0 \leqslant \beta \leqslant \beta_{1c}$) at each section $\zeta = \zeta_k$, we approximate the flow as being the flow over a circular cone with half angle $\theta_k = \tan^{-1}(f'(\beta = \beta_{1c}, \zeta = \zeta_k))$. We then compute the rest of the flow ($\beta > \beta_{1c}$) by integrating the (nonaxisymmtric) equations using the numerical scheme described above. Note that flow over a noncircular cone is constant along the shock and the body at each section $\zeta = \zeta_k$. Hence we compute the flow along the β direction until this constancy condition is met within a prescribed error tolerance.

Since many of the steps in our procedure are iterative, a good first approximation can significantly accelerate convergence. To motivate our choice of a first approximation observe that (17), (18), and (21) differ from axisymmetric flow in the "second order" terms,

$$\omega^2, \qquad \omega \frac{\partial}{\partial \phi}, \qquad \frac{\partial \omega}{\partial \phi},$$

where as (19) indicates, $\partial/\partial\phi = O(\partial/\partial\xi)$. Thus if a body can be regarded as locally axisymmetric taking the flow as axisymmetric should be an excellent approximation. In any case locally axisymmetric flow is the first approximation adopted by us.

4. Results and Discussions

For purposes of exposition we have performed calculations of flow over bodies with elliptical cross sections and azimuthal parabolic profiles. Relative few points, planes, and iterations are needed to compute the entire flow field. $\phi = 0$, π and $\phi = \pi/2$, $3\pi/2$ are planes of symmetry which are not assumed in the calculations, and are used as a check on the correctness of the results. Throughout the entire flow field, all grid points with such symmetry are found to have values in agreement within the same order of magnitude as the prescribed error tolerance.

Figure 3 shows the body and shock along the half planes $\phi = 0$ and $\phi = \pi$ for flow at $M_0 = 2$ over a body with 30% thickness at $\phi = 0$ and 20% thickness at $\phi = \pi/2$. To carry out this calculation we took 32 azimuthal sections each having 164 grid points, 20 on the body. The result of reducing the number of azimuthal planes to 16 is shown by x's and $+$'s. For calculations with the fine mesh size, the lines for $\phi = 0$ and $\phi = \pi$ are indistinguishable in this figure. For calculations with the coarse mesh size, $+$ signifies a point at $\phi = 0$ and $\times$ signifies a point at $\phi = \pi$. Each pair of $+$ and $\times$ appearing together in the figure have the same values of α and β, and hence they have the same flow values. Figure 4 shows the body and the shock for the same flow along $\phi = \pi/4$ and $\phi = 3\pi/4$. Again, for calculations with the fine mesh size, the lines for the two half planes are indistinguishable. For calculations with the coarse mesh size, $+$ signifies a point at $\phi = \pi/4$, and $\times$ signifies a point at $\phi = 3\pi/4$,

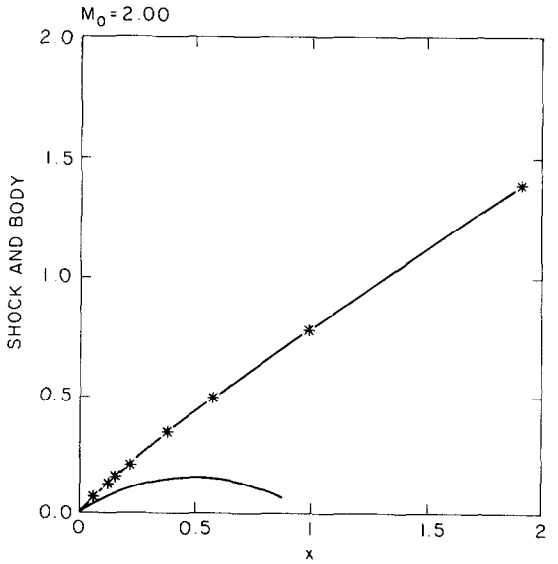

FIG. 3. Body and shock at $\phi = 0(+)$ and at $\phi = \pi(\times)$.

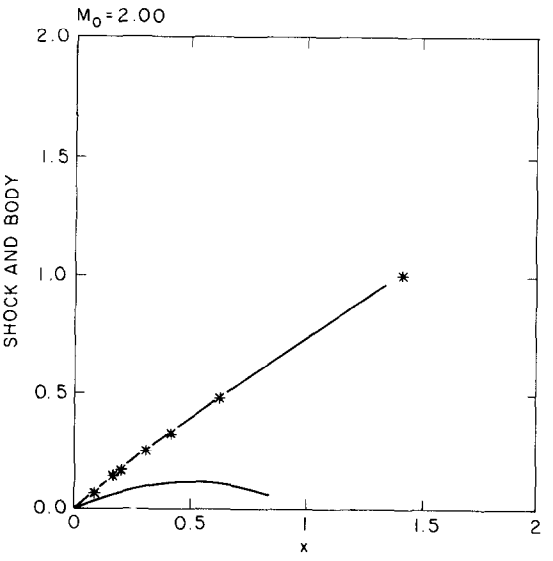

FIG. 4. Body and shock at $\phi = \pi/4(+)$ and at $\phi = 3\pi/4(\times)$.

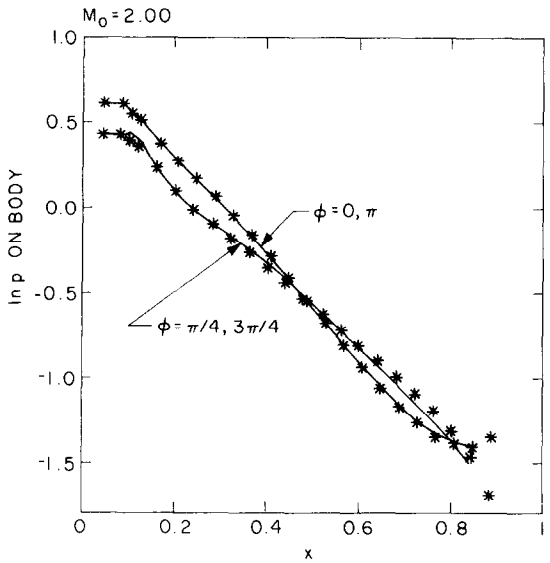

FIG. 5. Pressure distribution on the body. + is at $\phi = 0$ or $\pi/4$; × is at $\phi = 3\pi/4$ or π.

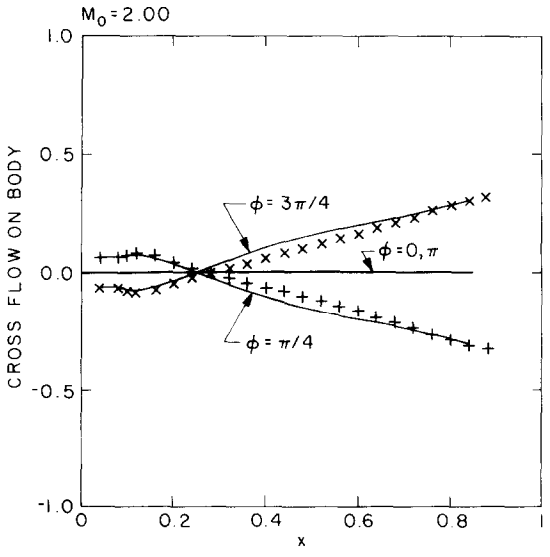

FIG. 6. Cross flow, normalized to $(u^2 + v^2)^{1/2}$, on the body.

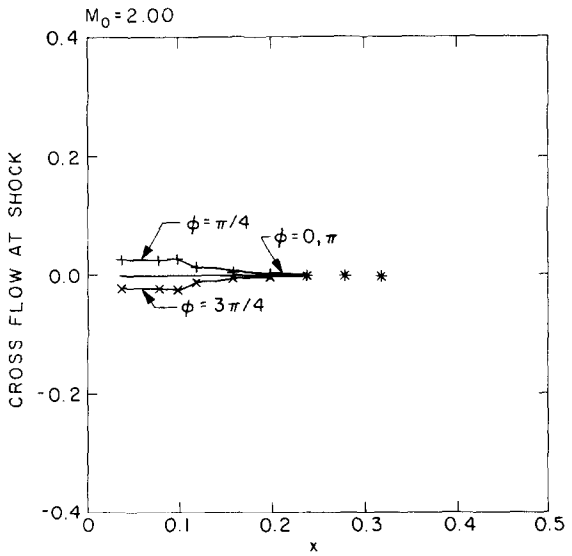

FIG. 7. Cross flow, normalized to $(u^2 + v^2)^{1/2}$, at the shock.

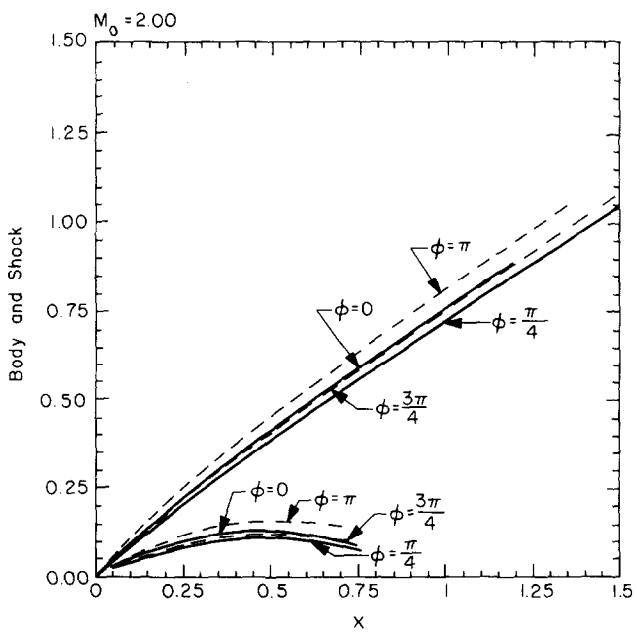

FIG. 8. Body and shock for flow at 2° angle of attack.

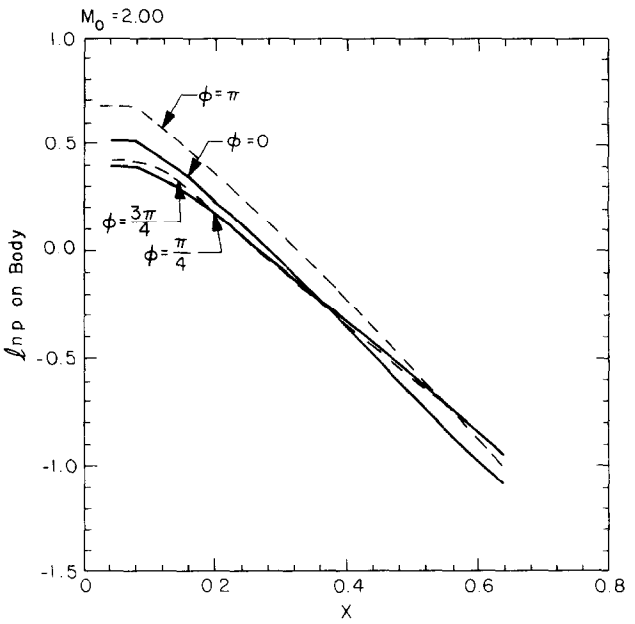

FIG. 9. Pressure distribution on the body for flow at 2 angle of attack.

with each pair of + and × having the same α and β. In these two figures, agreement is excellent with respect to both symmetry and the different grid sizes.

For the same flow, the pressure distribution on the body at $\phi = 0, \pi/4, \pi, 3\pi/4$ is shown in Fig. 5. For $\phi = 0, \pi$ the agreement is excellent. For $\phi = \pi/4, 3\pi/4$ the agreement is good with respect to symmetry, but there is a small discrepancy between the coarse and the fine grid calculations. Since the grid size in the ζ direction is quite large, about π/δ, the discrepancy is certainly tolerable.

The cross flow on the body is given in Fig. 6. As the figure shows, the cross flow vanishes in the symmetry plane. At $\phi = \pi/4, 3\pi/4$, there is some discrepancy between the coarse and fine grid calculations due to the largeness of the ζ grid size. Figure 7 shows that cross flow at the shock. The results are again quite good. Figures 8 and 9 show the same body at two degree angle of attack traveling at $M_0 = 2$.

As an indication of the computational speed, we mention that for the whose flow field, the time of a typical calculation is roughly 10 sec on an IBM 3081.

APPENDIX A. EQUATIONS IN NONAXISYMMETRIC FLOW

We wish to express the governing equations (1)–(7) in near characteristics form. Since $\rho = \rho(p, S)$, using (6) and (7), (1) becomes

$$\mathbf{u} \cdot \nabla p + \gamma p \nabla \cdot \mathbf{u} = 0. \tag{A1}$$

Denote

$$\mathbf{q} = (u, v) \qquad \text{and} \qquad \nabla_2 = \left(\frac{\partial}{\partial x}, \frac{\partial}{\partial r}\right).$$

Then (2) and (3) become

$$\mathbf{q} \cdot \nabla_2 \mathbf{q} + \frac{1}{\rho} \nabla_2 p = \mathbf{f}, \tag{A2}$$

where

$$\mathbf{f} = \frac{-w}{r} \frac{\partial}{\partial \phi} \mathbf{q} + \left(0, \frac{w^2}{r}\right).$$

In a constant half-plane with θ and μ defined by (8) and (9), let $\mathbf{t}(\theta)$ be the tangent, and $\mathbf{n}(\theta)$ be the normal on the projected streamline. Denote s and n as the arc length and normal coordinate. Then (A1) becomes

$$q \frac{\partial p}{\partial s} + \gamma p \left(\frac{\partial q}{\partial s} + q \frac{\partial \theta}{\partial n}\right) = -\left(\frac{w}{r} \frac{\partial p}{\partial \phi} + \frac{\gamma p v}{r} + \frac{\gamma p}{r} \frac{\partial w}{\partial \phi}\right), \tag{A3}$$

and (A2) becomes

$$q \frac{\partial q}{\partial s} + \frac{1}{\rho} \frac{\partial p}{\partial s} = \frac{-w}{r} \frac{\partial q}{\partial \phi} + \frac{w^2}{r} \sin \theta, \tag{A4}$$

$$q^2 \frac{\partial \theta}{\partial s} + \frac{1}{\rho} \frac{\partial p}{\partial n} = \frac{-wq}{r} \frac{\partial \theta}{\partial \phi} + \frac{w^2}{r} \cos \theta. \tag{A5}$$

Denote $\sigma = \ln p$ and $\omega = w/q$. Rearranging (A3), (A4), and (A5),

$$\left(\frac{\partial \theta}{\partial s} \pm \frac{1}{(M_*^2 - 1)^{1/2}} - \frac{\partial \theta}{\partial n}\right) \pm \frac{(M_*^2 - 1)^{1/2}}{\gamma M_*^2} \left(\frac{\partial \sigma}{\partial s} \pm \frac{1}{(M_*^2 - 1)^{1/2}} \frac{\partial \sigma}{\partial n}\right)$$
$$= F_1 \mp \frac{F_2}{(M_*^2 - 1)^{1/2}}, \tag{A6}$$

where $F_1 = (\omega^2/r) \cos \theta - (\omega/r)\, \theta_\phi$,

$$F_2 = \frac{1}{r} \omega_\phi + \frac{\omega}{\gamma r} \sigma_\phi + \frac{\sin \theta}{r} (1 + \omega^2).$$

(A6) can then be written as

$$d_\pm \theta \pm \frac{\sin 2\mu}{2\gamma} d_\pm \sigma = \frac{F_1 \cos \mu \mp F_2 \sin \mu}{\sin(\theta \pm \mu)} d_\pm r, \tag{A7}$$

where $d_\pm$ is given in (12).

Rewriting (5), we have

$$a^2 = \left(1 + \frac{\gamma - 1}{2}(M_0^2 - w^2)\right) \Big/ \left(1 + \frac{\gamma - 1}{2}\frac{1}{\sin^2 \mu}\right)$$

$$= \left(1 + \frac{\gamma - 1}{2} M_0^2\right) \Big/ \left(1 + \frac{\gamma - 1}{2}\frac{1 + \omega^2}{\sin^2 \mu}\right). \tag{A8}$$

Combining (6), (A8), and $\rho = \gamma p / a^2$, we then obtain (13). Rearranging (A8), we get

$$w^2 = \omega^2 \left(1 + \frac{\gamma - 1}{2} M_0^2\right) \Big/ \left(\sin^2 \mu + \frac{\gamma - 1}{2}(1 + \omega^2)\right).$$

Now define

$$W = \ln\left(1 + \frac{\gamma - 1}{2}(M_0^2 - w^2)\right). \tag{A9}$$

Since the derivative of the Prandtl function is

$$P'(\mu) = \cos^2 \mu \Big/ \left(\frac{\gamma - 1}{2} + \sin^2 \mu\right),$$

using (13), (A7) becomes (11) with

$$G_1 = \omega\left(\omega - \frac{\theta_\phi}{\cos \theta}\right), \tag{A10}$$

$$G_2 = \tan \mu \left(\omega^2 \tan \theta + \frac{\omega_\phi + (\omega/\gamma)\,\sigma_\phi}{\cos \theta}\right). \tag{A11}$$

Next, we wish to express the entropy equation (7) in a form useful to us. (7) can be written as

$$(\mathbf{q} \cdot \nabla_2)\, S + \frac{w}{r}\frac{\partial S}{\partial \phi} = 0.$$

In the natural coordinates s and n, this becomes

$$q \frac{\partial S}{\partial s} = \frac{-w}{r}\frac{\partial S}{\partial \phi}. \tag{A12}$$

If we define (α, β, ζ) by (14) and use the fact that s is the arc length, we get

$$\frac{\partial}{\partial s} = \frac{1}{(x_\beta^2 + r_\beta^2)^{1/2}}\frac{\partial}{\partial \beta} = \frac{1}{x_\beta (1 + \tan^2 \theta)^{1/2}}\frac{\partial}{\partial \beta} = \frac{\cos \theta}{x_\beta}\frac{\partial}{\partial \beta}. \tag{A13}$$

(A12) then becomes (21).

Now we give a similar treatment for the ϕ momentum equation (4). This can be written as

$$(\mathbf{q}\cdot\nabla_2)\,w+\frac{\gamma p}{\rho}\frac{1}{\gamma r p}\frac{\partial p}{\partial \phi}=\frac{-w}{r}\frac{\partial w}{\partial \phi}-\frac{vw}{r}.$$

In natural coordinates, this becomes

$$q\frac{\partial q\omega}{\partial s}+\frac{a^2}{\gamma r}\frac{\partial \sigma}{\partial \phi}=\frac{-q\omega}{r}\frac{\partial q\omega}{\partial \phi}-q^2\frac{\omega\sin\phi}{r}.$$

Using (A4) and (A13), this then becomes (22).

Appendix B. Coordinate Transformation

For $x=x(\alpha,\beta,\zeta)$, $r=r(\alpha,\beta,\zeta)$, $\phi=\phi(\alpha,\beta,\zeta)$, using the chain rule we obtain

$$\begin{pmatrix} x_\alpha & x_\beta & x_\zeta \\ r_\alpha & r_\beta & r_\zeta \\ \phi_\alpha & \phi_\beta & \phi_\zeta \end{pmatrix}\begin{pmatrix} \alpha_x & \alpha_r & \alpha_\phi \\ \beta_x & \beta_r & \beta_\phi \\ \zeta_x & \zeta_r & \zeta_\phi \end{pmatrix}=I.$$

Since $\phi=\zeta$, and $\phi_\alpha=\phi_\beta=0$, $\phi_\zeta=1$,

$$\begin{pmatrix} \alpha_x & \alpha_r & \alpha_\phi \\ \beta_x & \beta_r & \beta_\phi \\ \zeta_x & \zeta_r & \zeta_\phi \end{pmatrix}=\frac{1}{D}\begin{pmatrix} r_\beta & -x_\beta & 0 \\ -r_\alpha & x_\alpha & 0 \\ 0 & 0 & D \end{pmatrix}\begin{pmatrix} 1 & 0 & -x_\zeta \\ 0 & 1 & -r_\zeta \\ 0 & 0 & 1 \end{pmatrix},$$

where

$$D=x_\alpha r_\beta-r_\alpha x_\beta=(\tan\theta-\tan(\theta+\mu))\,x_\alpha x_\beta.$$

Then

$$\frac{\partial}{\partial x}=\alpha_x\frac{\partial}{\partial\alpha}+\beta_x\frac{\partial}{\partial\beta}=\frac{1}{D}\left(r_\beta\frac{\partial}{\partial\alpha}-r_\alpha\frac{\partial}{\partial\beta}\right),$$

$$\frac{\partial}{\partial r}=\alpha_r\frac{\partial}{\partial\alpha}+\beta_r\frac{\partial}{\partial\beta}=\frac{1}{D}\left(-x_\beta\frac{\partial}{\partial\alpha}+x_\alpha\frac{\partial}{\partial\beta}\right),$$

$$\begin{aligned}\frac{\partial}{\partial\phi}&=\alpha_\phi\frac{\partial}{\partial\alpha}+\beta_\phi\frac{\partial}{\partial\beta}+\zeta_\phi\frac{\partial}{\partial\zeta}\\&=\frac{(-r_\beta x_\zeta+x_\beta r_\zeta)(\partial/\partial\alpha)+(r_\alpha x_\zeta-x_\alpha r_\zeta)(\partial/\partial\beta)}{D}+\frac{\partial}{\partial\zeta}\\&=\frac{(r_\zeta-\tan\theta\,x_\zeta)\,x_\beta\,(\partial/\partial\alpha)+(\tan(\theta+\mu)\,x_\zeta-r_\zeta)\,x_\alpha(\partial/\partial\beta)}{D}+\frac{\partial}{\partial\zeta}.\end{aligned}$$

REFERENCES

1. M. HOLT, *Numerical Methods in Fluid Dynamics*, 2nd ed. (Springer–Verlag, New York, 1984).
2. R. PEYRET AND T. TAYLOR, *Computational Methods for Fluid Flow* (Springer–Verlag, New York, 1983).
3. R. RICHTMYER AND K. MORTON, *Difference Method for Initial Value Problem*, 2nd ed. (Wiley, New York, 1967).
4. M. CLINE AND J. HOFFMAN, *AIAA J.* **10**, 1452 (1972).
5. F. MARCONI, M. SALAS, AND L. YAEGER, NASA CR-2675, 1976 (unpublished).
6. G. MORETTI, B. GROSSMAN, AND F. MARCONI, *AIAA* Paper 72 (1972).
7. K. BABENKO, G. VOSKRESENSKII, A. LYUBIMOV, AND V. RUSANOV, NASA TT F-380, 1968, (unpublished).
8. C. FERRARI, *J. Aero Sci.* **16**, 411 (1949).
9. R. SAUER, *Numerische Mathematik* **5**, 55 (1963).
10. A. FERRI, *General Theory of High Speed Aerodynamics*, VI (Princeton Univ. Press, Princeton, N.J., 1954).
11. G. MORETTI, *AIAA J.* **1**, 2192 (1963).
12. J. RAKICH, NASA TN D-5341, 1969, (unpublished).
13. T. LEWIS AND L. SIROVICH, *J. Fluid Mech.* **112**, 265 (1981).
14. J. FONG AND L. SIROVICH, *AIAA J.* (May 1986).
15. M. LIEPMANN AND A. ROSHKO, *Elements of Gasdynamics* (Wiley, New York, 1957), p. 85.